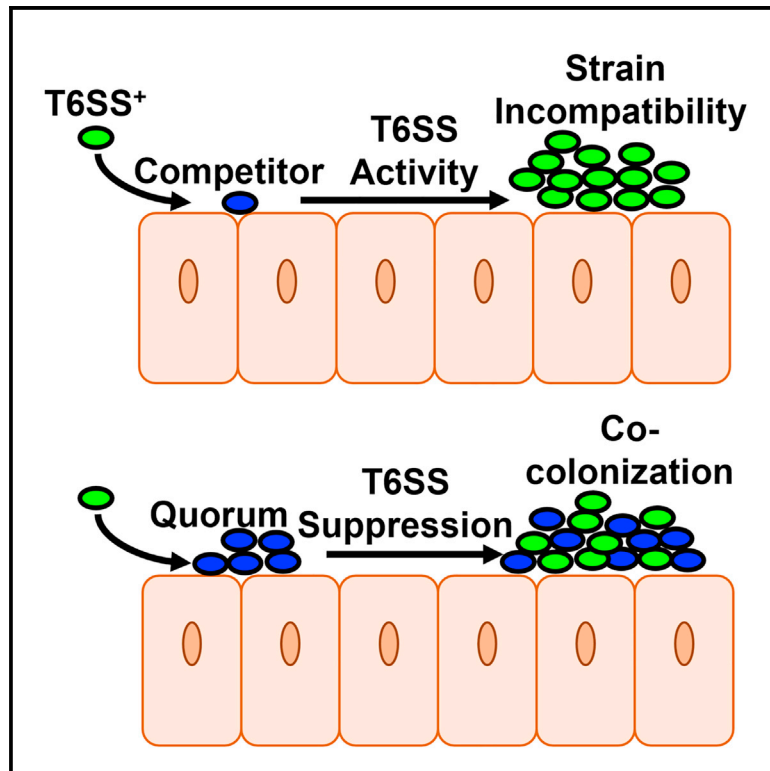


Current Biology

Quorum sensing inhibits interference competition among bacterial symbionts within a host

Graphical abstract



Authors

Kirsten R. Guckes, Taylor A. Yount, Caroline H. Steingard, Tim I. Miyashiro

Correspondence

tim14@psu.edu

In brief

Many bacterial symbionts encode interference competition mechanisms. Guckes et al. find that quorum sensing between bacterial symbionts suppresses an intercellular killing mechanism that promotes strain incompatibility within their squid host. This work provides insight into the multi-strain dynamics that take place during symbiosis establishment.

Highlights

- Quorum sensing inhibits type 6 secretion system (T6SS) activity in *Vibrio fischeri*
- Quorum-sensing regulator LitR downregulates the T6SS activator VasH
- Quorum sensing inhibits strain incompatibility during symbiosis establishment

Report

Quorum sensing inhibits interference competition among bacterial symbionts within a host

Kirsten R. Guckes,¹ Taylor A. Yount,¹ Caroline H. Steingard,¹ and Tim I. Miyashiro^{1,2,3,*}

¹Department of Biochemistry and Molecular Biology, The Pennsylvania State University, University Park, PA 16802, USA

²The One Health Microbiome Center, Huck Institutes of the Life Sciences, The Pennsylvania State University, University Park, PA 16802, USA

³Lead contact

*Correspondence: tim14@psu.edu

<https://doi.org/10.1016/j.cub.2023.08.051>

SUMMARY

The symbioses that animals form with bacteria play important roles in health and disease, but the molecular details underlying how bacterial symbionts initially assemble within a host remain unclear.^{1–3} The bioluminescent bacterium *Vibrio fischeri* establishes a light-emitting symbiosis with the Hawaiian bobtail squid *Euprymna scolopes* by colonizing specific epithelium-lined crypt spaces within a symbiotic organ called the light organ.⁴ Competition for these colonization sites occurs between different strains of *V. fischeri*, with the lancet-like type VI secretion system (T6SS) facilitating strong competitive interference that results in strain incompatibility within a crypt space.^{5,6} Although recent studies have identified regulators of this T6SS, how the T6SS is controlled as symbionts assemble *in vivo* remains unknown.^{7,8} Here, we show that T6SS activity is suppressed by *N*-octanoyl-L-homoserine lactone (C8 HSL), which is a signaling molecule that facilitates quorum sensing in *V. fischeri* and is important for efficient symbiont assembly.^{9,10} We find that this signaling depends on the quorum-sensing regulator LitR, which lowers expression of the needle subunit Hcp, a key component of the T6SS, by repressing transcription of the T6SS regulator VasH. We show that LitR-dependent quorum sensing inhibits strain incompatibility within the squid light organ. Collectively, these results provide new insights into the mechanisms by which regulatory networks that promote symbiosis also control competition among symbionts, which in turn may affect the overall symbiont diversity that assembles within a host.

RESULTS

Quorum sensing inhibits T6SS activity in *V. fischeri*

To establish symbiosis with *E. scolopes*, *V. fischeri* cells must access dedicated colonization sites (crypt spaces) within the light organ and then grow into light-emitting populations. Previous work has shown that the type VI secretion system (T6SS) encoded on the second chromosome of some *V. fischeri* strains (T6SS2) can prevent populations comprising certain strain combinations from forming within individual crypt spaces.¹¹ The main gene cluster encodes both the structural components of T6SS2 (Figure 1A) and at least one transcription factor that regulates its expression.⁷ However, how T6SS2 is regulated *in vivo* remains unclear, particularly as a population expands from a few founder cells to the carrying capacity of the crypt space.

To test whether T6SS2 activity changes as a population expands, we cultured FQ-A001, which is a T6SS2-positive strain, in rich medium and sampled the culture at different cell densities to assess cellular T6SS2 activity. As a negative control for T6SS2 activity, we used a strain lacking both *hcp* within the T6SS2 gene cluster and *hcp1* within an accessory T6SS2 gene cluster ($\Delta hcp \Delta hcp1$), which each encode identical copies of the Hcp subunit of the T6SS2 inner needle (Figure 1A).¹² To initially assess T6SS2 activity, we sampled a culture of FQ-A001 and co-incubated

those cells with CFP-labeled ES114, which is a T6SS2-negative strain susceptible to T6SS2-dependent killing. FQ-A001 cells derived from a culture grown overnight (ON) resulted in low CFP fluorescence in an Hcp-dependent manner (Figure 1B), consistent with FQ-A001 exhibiting T6SS activity as previously reported.⁷ While similar results were obtained with FQ-A001 cells harvested from a culture at low cell density (LCD; OD₆₀₀ ~0.2), cells grown to high cell density (HCD; OD₆₀₀ ~2.0) led to high CFP fluorescence that was comparable to the $\Delta hcp \Delta hcp1$ control (Figure 1B), which suggests low T6SS activity of FQ-A001 within the spot.

Previous work using an erythromycin-resistant (*erm*^R) strain of ES114 demonstrated that FQ-A001 kills ES114 cells within the first hours of their co-incubation in a T6SS2-dependent manner.¹² To investigate how growth physiology of FQ-A001 affects T6SS2-dependent killing, we tracked the abundance of *erm*^R ES114 within spots generated with FQ-A001 cells harvested from cultures at different growth phases. After 4 h of incubation with FQ-A001 cells collected from either ON and LCD cultures, *erm*^R ES114 CFU levels had decreased in an Hcp-dependent manner (Figures 1C and S1A). In contrast, *erm*^R ES114 grew after being incubated with FQ-A001 cells harvested from HCD cultures (Figures 1C and S1A), which suggests the harvested FQ-A001 cells had low T6SS2 activity. Further examination of FQ-A001 revealed a strong inverse correlation

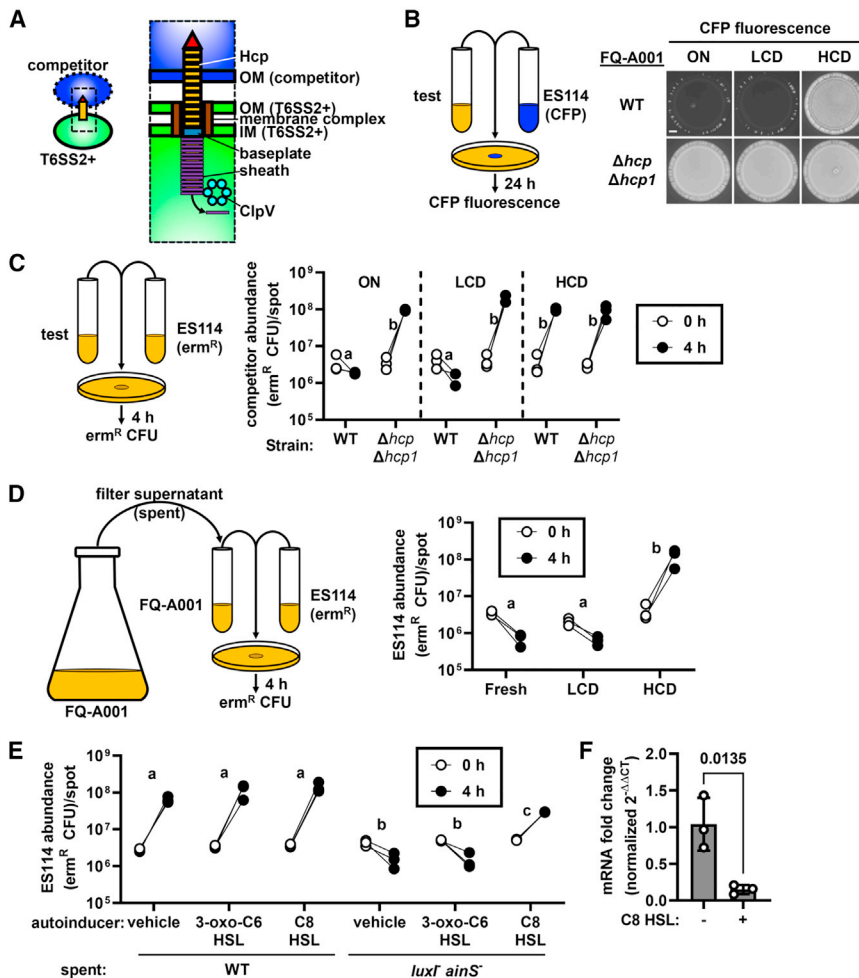


Figure 1. C8 HSL-mediated quorum sensing suppresses T6SS2 activity in *V. fischeri*

(A) T6SS2 structure. Mechanisms that control T6SS2 activity in *V. fischeri* are unknown. (B) Left: fluorescence-based co-incubation assay with FQ-A001-derived test and CFP-labeled ES114 competitor strains. Right: CFP fluorescence of spots with test strains grown overnight (ON), to low cell density (LCD), or to high cell density (HCD). Scale bar, 1 mm. (C) Left: co-incubation assay with test and *erm^R* ES114 competitor strains. Right: *erm^R* ES114 abundance within spots with FQ-A001-derived test strains grown as in (B). (D) Left: co-incubation assay with FQ-A001 cells incubated in spent media from FQ-A001 cultures. Right: *erm^R* ES114 abundance within spots with FQ-A001 grown in fresh or spent medium from cultures at LCD or HCD ($OD_{600} = 0.3$ and 2.5 , respectively). (E) *erm^R* ES114 abundance in spots with FQ-A001 cells grown in spent media from HCD cultures of ES114 wild-type and ES114 *luxI⁻ ainS⁻* ± indicated autoinducer ($1 \mu\text{M}$). (F) *hcp* transcript levels in FQ-A001 cultures at LCD $\pm 1 \mu\text{M}$ C8 HSL. Graphical and error bars = mean and SD. p value from t test. (C–E) Groups with identical (different) letters indicate same (different) statistical groups. See also [Figure S1](#) and [Data S1](#) for group statistics.

with C8 HSL but not *N*-3-oxohexanoyl-L-homoserine lactone (3-oxo-C6 HSL) suppressed FQ-A001 killing activity ([Figure 1E](#)). At $1 \mu\text{M}$, C8 HSL lowered transcription levels of the T6SS2 Hcp needle subunit 6.9-fold in FQ-A001 cells grown

to LCD ([Figure 1F](#)). Furthermore, promoter activity for each *hcp* gene decreased when FQ-A001 was grown on solid medium supplemented with C8 HSL ([Figure S1E](#)). Taken together, these data indicate that C8 HSL-mediated quorum sensing suppresses T6SS2 in *V. fischeri*.

between cell density and T6SS2 activity ([Figure S1B](#)), which suggests that T6SS2 activity is suppressed as a population grows. The observations described above led us to consider whether T6SS2 activity depends on quorum sensing, which is known to regulate T6SS in other *Vibrionaceae*.^{13–16} Quorum sensing occurs when self-produced signaling molecules (autoinducers) achieve a sufficient concentration in the environment to induce specific cellular responses throughout a population. FQ-A001 produces autoinducer at levels comparable to ES114 ([Figures S1C](#) and [S1D](#)), which has been reported to produce as much as $1.1 \mu\text{M}$ C8 HSL.¹⁷ To test whether the T6SS2 suppression is linked to autoinducer, we first generated spent media by filter-sterilizing supernatants of FQ-A001 cultures, then briefly exposed naive FQ-A001 cells to those spent media, and finally assessed their killing activity ([Figure 1D](#)). While spent media derived from LCD cultures had no effect on killing activity, the spent media generated from HCD cultures suppressed killing activity ([Figure 1D](#)). Spent media derived from LCD cultures of ES114 also suppressed FQ-A001 killing activity ([Figure 1E](#)), indicating T6SS2-negative strains also secrete the inhibitory product. In contrast, spent media generated from cultures of an ES114-derived mutant unable to produce HSL-based autoinducers (*luxI⁻ ainS⁻*) failed to suppress FQ-A001 killing activity ([Figure 1E](#)). However, supplementation of that spent medium

to LCD ([Figure 1F](#)). Furthermore, promoter activity for each *hcp* gene decreased when FQ-A001 was grown on solid medium supplemented with C8 HSL ([Figure S1E](#)). Taken together, these data indicate that C8 HSL-mediated quorum sensing suppresses T6SS2 in *V. fischeri*.

Quorum-sensing regulator LitR inhibits T6SS activity through Vash

The TetR-like transcription factor LitR is expressed when *V. fischeri* engages in C8 HSL-mediated quorum sensing ([Figure 2A](#)).¹⁸ In ES114, LitR is a global regulator that controls bioluminescence production, motility, and colony opacity, and it also contributes to the initial colonization of the light organ.^{19,20} To determine whether LitR also controls T6SS2 in *V. fischeri*, we tested the killing activity of a $\Delta litR$ strain of FQ-A001 and found it exhibited increased killing of ES114 even under HCD conditions ([Figure 2B](#)). Induction of *litR* expression in $\Delta litR$ in *trans* suppressed T6SS2 activity, thereby demonstrating genetic complementation ([Figure 2B](#)). Based on qRT-PCR, transcript levels of *hcp* were ~ 60 -fold higher in $\Delta litR$, which could be complemented by expressing *litR* in *trans* ([Figure 2C](#)). In addition, promoter activity for each *hcp* gene was elevated in the $\Delta litR$ mutant ([Figure S2A](#)). Together, these results suggest LitR represses T6SS2 expression.

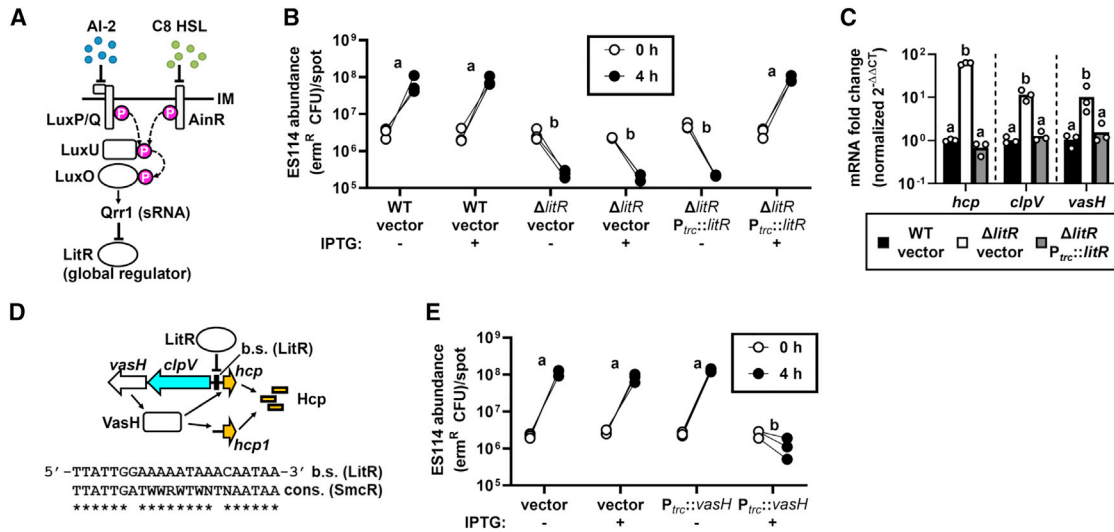


Figure 2. LitR inhibits T6SS activity via VasH

(A) C8 HSL-mediated quorum sensing promotes LitR expression by inhibiting the indicated phosphorelay.
 (B) erm^R ES114 abundance in spots with cells of indicated FQ-A001-derived strains grown in media \pm IPTG to HCD.
 (C) Levels of T6SS2 transcripts normalized to control *rpoD* in HCD-grown cells. Graphical bar = mean, with samples shown by points.
 (D) Schematic of LitR regulatory control over T6SS2 expression, with sequence of putative LitR binding site within the *clpV-hcp* intergenic region display.
 (E) erm^R ES114 abundance in spots with cells of FQ-A001 with IPTG-inducible *vasH* grown to HCD \pm IPTG.
 (B, C, and E) Groups with identical (different) letters indicate same (different) statistical groups.
 See also [Figure S2](#) and [Data S1](#) for group statistics.

To determine how LitR represses T6SS2 expression, we inspected the main and auxiliary T6SS2 gene clusters for putative LitR binding sites but identified only one centered 106 bp upstream of the *hcp* promoter (P_{hcp}) (Figure 2D).²¹ However, P_{hcp} is divergently transcribed from *clpV*, which indicates that the putative LitR binding site occurs within the intergenic region containing the promoter for *clpV* (P_{clpV}) (Figure 2D). This arrangement is notable because *vasH*, which encodes the bacterial enhancer binding protein that promotes σ^{54} -dependent transcription of both *hcp* genes,⁷ is located downstream of and is co-transcribed with *clpV* (Figures 2D and S2B). Similar to *hcp*, transcript levels of *clpV* and *vasH* are elevated in $\Delta litR$ (~10-fold), which suggests that LitR downregulates transcriptional expression of the VasH regulator (Figure 2C). To test whether ectopic expression of VasH could overcome T6SS2 suppression, we induced expression of *vasH* in FQ-A001 cells grown to HCD and observed increased killing of ES114 (Figure 2E), which suggests that the suppression of T6SS2 by LitR is due to low levels of VasH. Taken together, these results suggest that the T6SS2 of *V. fischeri* is suppressed by quorum sensing due to LitR repression of VasH.

Quorum sensing inhibits strain incompatibility during symbiosis establishment

In the *E. scolopes-V. fischeri* symbiosis, strain incompatibility describes the inability of different strains to colonize the same crypt space within a light organ,²² and previous work has established a dual-strain squid-colonization assay based on FQ-A001 and ES114 to experimentally study this phenomenon.^{7,11,12} Briefly, juvenile squid are first exposed to an inoculum containing FQ-A001 and ES114 labeled with different fluorescent proteins,

and then their light organs are assessed by fluorescence microscopy at 24 h post-inoculation (p.i.) to score the crypt spaces for each strain (Figures 3A and 3B). To determine whether quorum sensing impacts strain incompatibility, we treated juvenile squid with 1 μ M C8 HSL directly after completion of the 3.5-h inoculation stage and found that 4/26 (15%) animals featured at least one crypt space containing both strains in contrast to none of the animals in the control group ($p = 0.04136$, two-tailed two-proportion Z test) (Figure 3C), which suggests that C8 HSL can inhibit strain incompatibility within crypt spaces. To test whether this effect depends on LitR, we examined animals treated with 1 μ M C8 HSL following exposure to an inoculum containing FQ-A001 $\Delta litR$ and ES114. We found that none of the animals had co-colonized crypts in contrast to the 13/21 (62%) animals in the control group featuring FQ-A001 ($p < 0.00001$, two-tailed, two-proportion Z test) (Figure 3D), which suggests that strain incompatibility occurs with $\Delta litR$ and ES114 despite the presence of C8 HSL. Taken together, these results suggest that the ability of C8 HSL to inhibit strain incompatibility within the light organ depends on FQ-A001 encoding LitR.

Previous work has shown that strains related to FQ-A001 tend to enter crypt spaces more quickly than ES114.²³ Therefore, we hypothesized that in a crypt accessed by both strains, strain incompatibility occurs before the population grows sufficiently large to engage in C8 HSL-mediated quorum sensing. To test this hypothesis, we exposed animals first to ES114 and then to FQ-A001 after a 1-h delay and found that 15/26 (58%) animals had at least one crypt space containing both strains in contrast to the control group that featured no co-colonized crypts ($p < 0.0001$, two-tailed, two-proportion Z test) (Figure 3E), which suggests that early entry of ES114 to a crypt space can inhibit

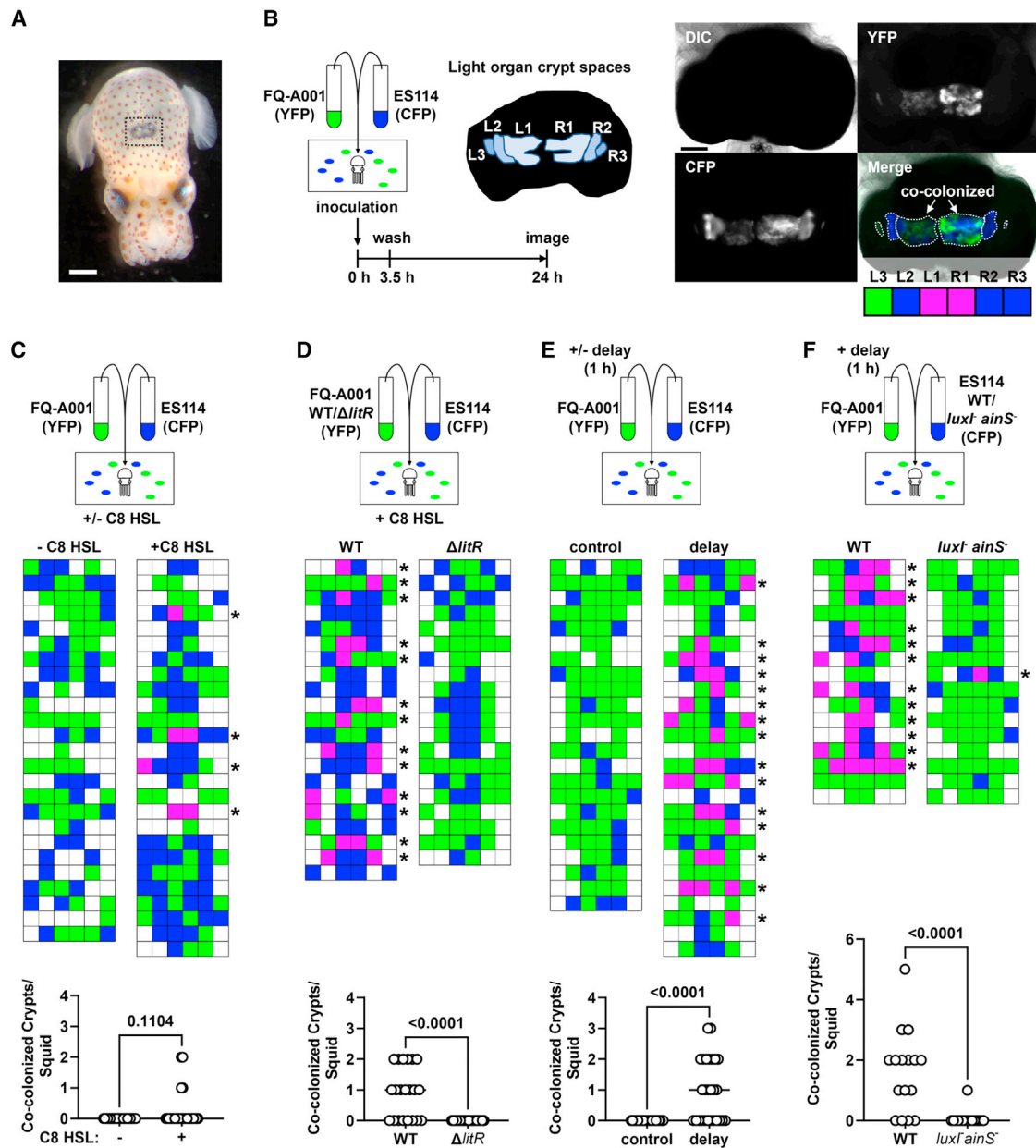


Figure 3. Quorum sensing inhibits strain incompatibility during symbiosis establishment

(A) Juvenile *E. scolopes*, with box highlighting light organ. Scale bar, 0.5 mm.
 (B) Left: experimental design to assess T6SS2-dependent strain incompatibility between FQ-A001 (YFP) and ES114 (CFP) *in vivo*. Right: images of light organ featuring colonized crypt spaces, with corresponding scoring metric. Scale bar, 100 μ m.
 (C) Colonization assay performed \pm 1 μ M C8 HSL, with animals featuring ≥ 1 co-colonized crypt space labeled with asterisk.
 (D) Colonization assay performed with 1 μ M C8 HSL with FQ-A001-derived wild-type or $\Delta litR$ strains, with animals featuring ≥ 1 co-colonized crypt space labeled with asterisk.
 (E) Colonization assay performed with a 1-h delay in FQ-A001 inoculation, with animals featuring ≥ 1 co-colonized crypt space labeled with asterisk.
 (F) Colonization assay performed with ES114-derived wild-type or *luxI⁻ ainS⁻* strains and a 1-h delay in FQ-A001 inoculation, with animals featuring ≥ 1 co-colonized crypt space labeled with asterisk.
 (C–F) Bars = medians. Each p value corresponds to an unpaired Mann-Whitney test.

strain incompatibility with FQ-A001. To determine whether the ability of ES114 to produce HSL-based autoinducers impacts this effect, we used the *luxI⁻ ainS⁻* mutant of ES114 and again delayed the introduction of FQ-A001 into the inoculum by 1 h.

In contrast to the wild-type control that featured 12/16 (75%) animals with co-colonized crypt spaces, the group involving the ES114-derived mutant had only one animal with a single co-colonized crypt space ($p = 0.00008$, two-tailed, two-proportion

Z test) (Figure 3F), which suggests that the ability to produce HSL-based autoinducers is important for ES114 to occupy the same crypt space as FQ-A001. Taken together, these experiments suggest that C8 HSL-mediated quorum sensing can inhibit strain incompatibility in *V. fischeri* and that the initial assembly dynamics play a critical role in determining how different strains interact while establishing symbiosis.

DISCUSSION

Recent findings indicate that interbacterial competition plays an important role in animal-bacterial symbioses by dictating which symbionts are sufficiently abundant to function *in vivo*.^{11,24–26} However, the mechanisms by which bacterial symbionts regulate the genetic factors that govern competition have remained unclear. In this study, we have shown that C8 HSL-based quorum sensing inhibits expression of the VasH regulator via the transcription factor LitR in *V. fischeri*. This regulation lowers expression of Hcp, which prevents T6SS-dependent bacterial killing of other symbiotic strains.

We observed an anticorrelation between cell density and T6SS2 activity in *V. fischeri* that is due to regulation of Hcp expression at the level of transcription. A previous study suggested that transcriptional expression of Hcp is elevated when *V. fischeri* is grown on solid surfaces or in high-viscosity liquid environments but not in low-viscosity liquid environments.²⁷ Notably, those experiments required the liquid-based cultures to grow for 12 h. Based on the findings reported here (Figures 1C, 1F, and 2C), those cultures had likely established a quorum so that LitR repressed transcription of the *hcp* genes, inadvertently leading to the incorrect conclusion that T6SS2 activity does not occur in low-viscosity liquid. Instead, our results suggest that *V. fischeri* expresses the T6SS2 system in aqueous environments unless Hcp expression is suppressed by cells engaging in C8 HSL-based quorum sensing. How C8 HSL-based quorum sensing affects viscosity-dependent intercellular interactions remains unknown and is an important direction for future studies.

Our previous studies that investigated the molecular underpinnings of T6SS2 benefited from the fact that ON cultures exhibit T6SS2 activity, which is curious given the discovery reported here that HCD conditions suppress T6SS2.^{7,12} One possibility is that the environmental conditions associated with ON cultures lower the stability of autoinducers as observed for other bacteria.^{28,29} The low levels of C8 HSL would promote expression of the small regulatory RNA Qrr1 that post-transcriptionally inhibits LitR,^{30,31} thereby permitting T6SS2 to be transcribed. Alternatively, *V. fischeri* may encode another regulatory factor that overrides LitR repression to activate the T6SS2 gene expression during late stationary phase. Further studies are necessary to address how the differences in cell physiology between ON and HCD conditions alter T6SS2 activity.

High Hcp expression is paramount for cells to maintain T6SS-mediated aggression.³² In general, the stoichiometry of a T6SS requires up to 700 copies of Hcp per complex.³³ Furthermore, because the inner tube is lost to the environment upon each firing event, Hcp must be synthesized *de novo* for an individual complex to function again. Among T6SS gene clusters in *V. fischeri*, only the *hcp* operons depend on σ^{54} for transcriptional activation,^{5,7} which is a regulatory architecture that has

been shown in other T6SS-positive bacteria to permit the differential expression of secreted components relative to the components of the membrane complex and sheath.³⁴ In *V. fischeri*, the main gene cluster contains one of the *hcp* genes,¹² which is different than in some other *Vibrionaceae* that possess *hcp* genes only within auxiliary gene clusters with nearly identical promoter regions, e.g., *V. cholerae*.³⁴ How the specific arrangement of the two *hcp* genes in *V. fischeri* impacts the dynamics of T6SS will be the focus of future investigations.

Our discovery that quorum sensing can lower T6SS activity in *V. fischeri* has major implications for whether strain incompatibility will occur within the squid light organ. For instance, if a strain can establish a quorum within a crypt space prior to the entry of an incompatible T6SS-positive cell, then the corresponding C8 HSL will likely dampen T6SS activity of the secondary colonizer, which inhibits interference competition to permit the occurrence of a mixed population. Consequently, our finding of conditions that result in crypt spaces co-colonized with ES114 and FQ-A001 illustrates a striking example of an inhibitory priority effect, in which the production of C8 HSL by the primary colonizer alters the habitat in a way that allows greater strain diversity during the initial colonization of the light organ. Colonization of a crypt space leads to that space becoming recalcitrant to subsequent colonization events due to constriction of the crypt-specific duct within 6–24 h, so that the strains that successfully colonize the host during the first few hours after hatching are the only ones that can be maintained throughout the life history of the squid.³⁵ Thus, this regulatory mechanism that operates within this critical window of time may explain how both T6SS-positive and T6SS-negative strains are frequently recovered from individual wild-caught squid.¹¹ Future work will hone in on this period of time to directly test the extent to which LitR controls T6SS2 expression *in vivo*.

The ability of *V. fischeri* to regulate T6SS activity by quorum sensing enables a specific bacterial signal to alter how microbes interact with one another in specific environments. Our observation is reminiscent of how quorum sensing influences the interactions among *V. cholerae* cells that are growing on the chitin-rich exoskeletons of zooplankton.^{36,37} By expressing chitinases that break down the otherwise insoluble chitin polymers, *V. cholerae* releases smaller chains of *N*-acetylglucosamine that stimulate the natural transformation pathway.³⁸ Under conditions of HCD, quorum sensing upregulates Hcp expression via HapR, which contributes to increased T6SS activity.¹³ Consequently, quorum sensing on chitinous surfaces enables *V. cholerae* to lyse neighboring cells via effectors delivered by T6SS, which releases large fragments of DNA that can be incorporated by natural transformation.³⁹ Our discovery that *V. fischeri* responds to quorum sensing in an opposite manner, i.e., by suppressing T6SS expression, underscores how the ecological niche of a microbe drives the evolution of its T6SS. Thus, an understanding of the spatiotemporal dynamics of T6SS activity for the *V. fischeri* populations within the light organ will be an important direction for future research. Recent work has shown that the different populations within the light organ can interact via quorum sensing such that 3-oxo-C6 HSL synthesized by one population can induce bioluminescence production by cells in neighboring crypt spaces.⁴⁰ Whether C8 HSL can also facilitate interpopulation signaling and perhaps mediate the suppression of T6SS activity from a distance remains to be seen.

While we have shown that LitR downregulates T6SS activity through VasH, we expect other traits of FQ-A001 that affect the symbiosis to be regulated by quorum sensing independent of VasH. In ES114, it is well established that LitR regulates bioluminescence production, motility, and colony opacity, and this global regulator also contributes to the initial colonization of the light organ.^{19,20} Our finding that the LitR regulon can include T6SS-related genes suggests that this regulatory network can be re-purposed in different symbiotic strains. Further work is needed to determine the extent to which the regulatory network of LitR has been re-wired in different strains and how these modifications impact symbiosis establishment.

The ability of LitR to suppress T6SS activity may highlight a cost to fitness if T6SS expression is left unchecked. In addition to cells needing to resynthesize the inner tube *de novo* after each firing event as described above, they must also unfold the sheath subunits through a dedicated ATPase to recycle the T6SS membrane complex.⁴¹ One possibility is that when coupled with bioluminescence production, the energetics associated with a constitutive T6SS would be too high for the energy captured from fermentation of chitin-derived oligosaccharides supplied by the squid host to maintain the symbiont population at night.⁴² Conversely, there may be a benefit of a multi-strain population inhabiting a crypt space that impacts the symbiosis. The remarkable amenability of the *E. scolopes-V. fischeri* system to experimental manipulation makes the pursuit of such inquiries feasible. In summary, an understanding of the regulatory mechanisms of cellular aggression in a bacterial symbiont, such as the example reported here, provides important insight into the role of intercellular interactions in the dynamics of symbiont assembly during the initial steps of host colonization.

STAR★METHODS

Detailed methods are provided in the online version of this paper and include the following:

- **KEY RESOURCES TABLE**
- **RESOURCE AVAILABILITY**
 - Lead contact
 - Materials availability
 - Data and code availability
- **EXPERIMENTAL MODEL AND SUBJECT DETAILS**
 - Growth conditions
- **METHOD DETAILS**
 - Molecular Biology
 - Co-incubation assays
 - Bioluminescence assay
 - Reverse transcriptase-Quantitative PCR (RT-qPCR)
 - GFP-based promoter reporter assays
 - Endpoint RT-PCR
 - Squid-colonization assays
- **QUANTIFICATION AND STATISTICAL ANALYSIS**

SUPPLEMENTAL INFORMATION

Supplemental information can be found online at <https://doi.org/10.1016/j.cub.2023.08.051>.

ACKNOWLEDGMENTS

This work was supported by National Institute of General Medical Sciences grant R01 GM129133 (to T.I.M.), National Institute of Allergy and Infectious Diseases Fellowship F32 AI147543 (to K.R.G.), and Beckman Scholars Program award (to T.A.Y.). The authors also thank the outstanding feedback of three anonymous reviewers during the peer-review process.

AUTHOR CONTRIBUTIONS

Conceptualization, K.R.G. and T.I.M.; investigation, K.R.G., T.A.Y., C.H.S., and T.I.M.; methodology, K.R.G. and T.I.M.; writing – original draft, K.R.G.; writing – review & editing, K.R.G. and T.I.M.; funding acquisition, K.R.G. and T.I.M.

DECLARATION OF INTERESTS

The authors declare no competing interests.

INCLUSION AND DIVERSITY

We support inclusive, diverse, and equitable conduct of research.

Received: March 9, 2023

Revised: June 20, 2023

Accepted: August 16, 2023

Published: September 8, 2023

REFERENCES

1. McFall-Ngai, M., Hadfield, M.G., Bosch, T.C.G., Carey, H.V., Domazet-Lošo, T., Douglas, A.E., Dubilier, N., Eberl, G., Fukami, T., Gilbert, S.F., et al. (2013). Animals in a bacterial world, a new imperative for the life sciences. *Proc. Natl. Acad. Sci. USA* *110*, 3229–3236. <https://doi.org/10.1073/pnas.1218525110>.
2. Moran, N.A. (2006). Symbiosis. *Curr. Biol.* *16*, R866–R871. <https://doi.org/10.1016/j.cub.2006.09.019>.
3. Ganesan, R., Wierz, J.C., Kaltenpoth, M., and Flórez, L.V. (2022). How it all begins: bacterial factors mediating the colonization of invertebrate hosts by beneficial symbionts. *Microbiol. Mol. Biol. Rev.* *86*, e0012621, <https://doi.org/10.1128/mbr.00126-21>.
4. Visick, K.L., Stabb, E.V., and Ruby, E.G. (2021). A lasting symbiosis: how *Vibrio fischeri* finds a squid partner and persists within its natural host. *Nat. Rev. Microbiol.* *19*, 654–665. <https://doi.org/10.1038/s41579-021-00557-0>.
5. Guckes, K.R., and Miyashiro, T.I. (2023). The type-VI secretion system of the beneficial symbiont *Vibrio fischeri*. *Microbiology (Read.)* *169*, 001302, <https://doi.org/10.1099/mic.0.001302>.
6. Bongrand, C., and Ruby, E.G. (2019). The impact of *Vibrio fischeri* strain variation on host colonization. *Curr. Opin. Microbiol.* *50*, 15–19. <https://doi.org/10.1016/j.mib.2019.09.002>.
7. Guckes, K.R., Cecere, A.G., Williams, A.L., McNeil, A.E., and Miyashiro, T. (2020). The bacterial enhancer binding protein VasH promotes expression of a type VI secretion system in *Vibrio fischeri* during symbiosis. *J. Bacteriol.* *202*, 007777–19. <https://doi.org/10.1128/JB.00777-19>.
8. Smith, S., Salvato, F., Garikipati, A., Kleiner, M., and Septer, A.N. (2021). Activation of the type VI secretion system in the squid symbiont *Vibrio fischeri* requires the transcriptional regulator TasR and the structural proteins TssM and TssA. *J. Bacteriol.* *203*, e0039921, <https://doi.org/10.1128/JB.00399-21>.
9. Verma, S.C., and Miyashiro, T. (2013). Quorum sensing in the squid-*Vibrio* symbiosis. *Int. J. Mol. Sci.* *14*, 16386–16401. <https://doi.org/10.3390/ijms140816386>.
10. Miyashiro, T., and Ruby, E.G. (2012). Shedding light on bioluminescence regulation in *Vibrio fischeri*. *Mol. Microbiol.* *84*, 795–806. <https://doi.org/10.1111/j.1365-2958.2012.08065.x>.

- Speare, L., Cecere, A.G., Guckes, K.R., Smith, S., Wollenberg, M.S., Mandel, M.J., Miyashiro, T., and Septer, A.N. (2018). Bacterial symbionts use a type VI secretion system to eliminate competitors in their natural host. *Proc. Natl. Acad. Sci. USA* *115*, E8528–E8537. <https://doi.org/10.1073/pnas.1808302115>.
- Guckes, K.R., Cecere, A.G., Wasilko, N.P., Williams, A.L., Bultman, K.M., Mandel, M.J., and Miyashiro, T. (2019). Incompatibility of *Vibrio fischeri* strains during symbiosis establishment depends on two functionally redundant *hcp* genes. *J. Bacteriol.* *201*, e00221002211–19. <https://doi.org/10.1128/JB.00221-19>.
- Shao, Y., and Bassler, B.L. (2014). Quorum regulatory small RNAs repress type VI secretion in *Vibrio cholerae*. *Mol. Microbiol.* *92*, 921–930. <https://doi.org/10.1111/mmi.12599>.
- Salomon, D., Gonzalez, H., Updegraff, B.L., and Orth, K. (2013). *Vibrio parahaemolyticus* type VI secretion system 1 is activated in marine conditions to target bacteria, and is differentially regulated from system 2. *PLoS One* *8*, e61086. <https://doi.org/10.1371/journal.pone.0061086>.
- Sheng, L., Gu, D., Wang, Q., Liu, Q., and Zhang, Y. (2012). Quorum sensing and alternative sigma factor RpoN regulate type VI secretion system I (T6SSVA1) in fish pathogen *Vibrio alginolyticus*. *Arch. Microbiol.* *194*, 379–390. <https://doi.org/10.1007/s00203-011-0780-z>.
- Liu, X., Pan, J., Gao, H., Han, Y., Zhang, A., Huang, Y., Liu, P., Kan, B., and Liang, W. (2021). CqsA/LuxS-HapR quorum sensing circuit modulates type VI secretion system V fl T6SS2 in *Vibrio fluvialis*. *Emerg. Microbes Infect.* *10*, 589–601. <https://doi.org/10.1080/22221751.2021.1902244>.
- Girard, L., Blanchet, E., Stien, D., Baudart, J., Suzuki, M., and Lami, R. (2019). Evidence of a large diversity of N-acyl-homoserine lactones in symbiotic *Vibrio fischeri* strains associated with the squid *Euprymna scolopes*. *Microbes Environ.* *34*, 99–103. <https://doi.org/10.1264/jsme2.ME18145>.
- Miyashiro, T., Wollenberg, M.S., Cao, X., Oehlert, D., and Ruby, E.G. (2010). A single *qrr* gene is necessary and sufficient for LuxO-mediated regulation in *Vibrio fischeri*. *Mol. Microbiol.* *77*, 1556–1567. <https://doi.org/10.1111/j.1365-2958.2010.07309.x>.
- Fidopiastis, P.M., Miyamoto, C.M., Jobling, M.G., Meighen, E.A., and Ruby, E.G. (2002). LitR, a new transcriptional activator in *Vibrio fischeri*, regulates luminescence and symbiotic light organ colonization. *Mol. Microbiol.* *45*, 131–143.
- Lupp, C., and Ruby, E.G. (2005). *Vibrio fischeri* uses two quorum-sensing systems for the regulation of early and late colonization factors. *J. Bacteriol.* *187*, 3620–3629. <https://doi.org/10.1128/JB.187.11.3620-3629.2005>.
- Lee, D.H., Jeong, H.S., Jeong, H.G., Kim, K.M., Kim, H., and Choi, S.H. (2008). A consensus sequence for binding of SmcR, a *Vibrio vulnificus* LuxR homologue, and genome-wide identification of the SmcR regulon. *J. Biol. Chem.* *283*, 23610–23618. <https://doi.org/10.1074/jbc.M801480200>.
- Sun, Y., LaSota, E.D., Cecere, A.G., LaPenna, K.B., Larios-Valencia, J., Wollenberg, M.S., and Miyashiro, T. (2016). Intraspecific competition impacts *Vibrio fischeri* strain diversity during initial colonization of the squid light organ. *Appl. Environ. Microbiol.* *82*, 3082–3091. <https://doi.org/10.1128/AEM.04143-15>.
- Bongrand, C., and Ruby, E.G. (2019). Achieving a multi-strain symbiosis: strain behavior and infection dynamics. *ISME J.* *13*, 698–706. <https://doi.org/10.1038/s41396-018-0305-8>.
- Steele, M.I., Kwong, W.K., Whiteley, M., and Moran, N.A. (2017). Diversification of type VI secretion system toxins reveals ancient antagonism among bee. *mBio* *8*, e01630-17. <https://doi.org/10.1128/mBio.01630-17>.
- Verster, A.J., Ross, B.D., Radey, M.C., Bao, Y., Goodman, A.L., Mougous, J.D., and Borenstein, E. (2017). The landscape of type VI secretion across human gut microbiomes reveals its role in community composition. *Cell Host Microbe* *22*, 411–419.e4. <https://doi.org/10.1016/j.chom.2017.08.010>.
- Kochanowsky, R.M., Bradshaw, C., Forlastro, I., and Stock, S.P. (2020). *Xenorhabdus bovienii* strain jolietti uses a type 6 secretion system to kill closely related *Xenorhabdus* strains. *FEMS Microbiol. Ecol.* *96*, fiae073. <https://doi.org/10.1093/femsec/fiae073>.
- Speare, L., Smith, S., Salvato, F., Kleiner, M., and Septer, A.N. (2020). Environmental viscosity modulates interbacterial killing during habitat transition. *mBio* *11*, e03060-19. <https://doi.org/10.1128/mBio.03060-19>.
- Yates, E.A., Philipp, B., Buckley, C., Atkinson, S., Chhabra, S.R., Sockett, R.E., Goldner, M., Dessaux, Y., Cámara, M., Smith, H., and Williams, P. (2002). N-acylhomoserine lactones undergo lactonolysis in a pH-temperature- and acyl chain length-dependent manner during growth of *Yersinia pseudotuberculosis* and *Pseudomonas aeruginosa*. *Infect. Immun.* *70*, 5635–5646. <https://doi.org/10.1128/IAI.70.10.5635-5646.2002>.
- Byers, J.T., Lucas, C., Salmond, G.P.C., and Welch, M. (2002). Nonenzymatic turnover of an *Erwinia carotovora* quorum-sensing signaling molecule. *J. Bacteriol.* *184*, 1163–1171. <https://doi.org/10.1128/jb.184.4.1163-1171.2002>.
- Kimbrough, J.H., and Stabb, E.V. (2013). Substrate specificity and function of the pheromone receptor AinR in *Vibrio fischeri* ES114. *J. Bacteriol.* *195*, 5223–5232. <https://doi.org/10.1128/JB.00913-13>.
- Surrett, E.D., Guckes, K.R., Cousins, S., Ruskoski, T.B., Cecere, A.G., Ludvik, D.A., Okafor, C.D., Mandel, M.J., and Miyashiro, T.I. (2023). Two enhancer binding proteins activate sigma(54)-dependent transcription of a quorum regulatory RNA in a bacterial symbiont. *eLife* *12*, e78544. <https://doi.org/10.7554/eLife.78544>.
- Lin, L., Lezan, E., Schmidt, A., and Basler, M. (2019). Abundance of bacterial type VI secretion system components measured by targeted proteomics. *Nat. Commun.* *10*, 2584. <https://doi.org/10.1038/s41467-019-10466-9>.
- Basler, M. (2015). Type VI secretion system: secretion by a contractile nanomachine. *Philos. Trans. R. Soc. Lond. B Biol. Sci.* *370*, 20150021. <https://doi.org/10.1098/rstb.2015.0021>.
- Seibt, H., Aung, K.M., Ishikawa, T., Sjöström, A., Gullberg, M., Atkinson, G.C., Wai, S.N., and Shingler, V. (2020). Elevated levels of VCA0117 (Vash) in response to external signals activate the type VI secretion system of *Vibrio cholerae* O1 El Tor A1552. *Environ. Microbiol.* *22*, 4409–4423. <https://doi.org/10.1111/1462-2920.15141>.
- Essock-Burns, T., Bongrand, C., Goldman, W.E., Ruby, E.G., and McFall-Ngai, M.J. (2020). Interactions of symbiotic partners drive the development of a complex biogeography in the squid-Vibrio symbiosis. *mBio* *11*, e00853008533-20. <https://doi.org/10.1128/mBio.00853-20>.
- Crisan, C.V., and Hammer, B.K. (2020). The *Vibrio cholerae* type VI secretion system: toxins, regulators and consequences. *Environ. Microbiol.* *22*, 4112–4122. <https://doi.org/10.1111/1462-2920.14976>.
- Veening, J.W., and Blokesch, M. (2017). Interbacterial predation as a strategy for DNA acquisition in naturally competent bacteria. *Nat. Rev. Microbiol.* *15*, 629. <https://doi.org/10.1038/nrmicro.2017.89>.
- Meibom, K.L., Blokesch, M., Dolganov, N.A., Wu, C.Y., and Schoolnik, G.K. (2005). Chitin induces natural competence in *Vibrio cholerae*. *Science* *310*, 1824–1827. <https://doi.org/10.1126/science.1120096>.
- Matthey, N., Stutzmann, S., Stoudmann, C., Guex, N., Iseli, C., and Blokesch, M. (2019). Neighbor predation linked to natural competence fosters the transfer of large genomic regions in *Vibrio cholerae*. *eLife* *8*, e48212. <https://doi.org/10.7554/eLife.48212>.
- Yount, T.A., Murtha, A.N., Cecere, A.G., and Miyashiro, T.I. (2022). Quorum sensing facilitates interpopulation signaling by *Vibrio fischeri* within the light organ of *Euprymna scolopes*. *Isr. J. Chem.* *63*, e202200061. <https://doi.org/10.1002/ijch.202200061>.
- Basler, M., and Mekalanos, J.J. (2012). Type 6 secretion dynamics within and between bacterial cells. *Science* *337*, 815. <https://doi.org/10.1126/science.1222901>.
- Schwartzman, J.A., Koch, E., Heath-Heckman, E.A.C., Zhou, L., Kremer, N., McFall-Ngai, M.J., and Ruby, E.G. (2015). The chemistry of negotiation: rhythmic, glycan-driven acidification in a symbiotic conversation. *Proc. Natl. Acad. Sci. USA* *112*, 566–571. <https://doi.org/10.1073/pnas.1418580112>.

43. Boettcher, K.J., and Ruby, E.G. (1990). Depressed light emission by symbiotic *Vibrio fischeri* of the sepiolid squid *Euprymna scolopes*. *J. Bacteriol.* *172*, 3701–3706.
44. Mandel, M.J., Stabb, E.V., and Ruby, E.G. (2008). Comparative genomics-based investigation of resequencing targets in *Vibrio fischeri*: focus on point miscalls and artefactual expansions. *BMC Genom.* *9*, 138. <https://doi.org/10.1186/1471-2164-9-138>.
45. Bultman, K.M., Cecere, A.G., Miyashiro, T., Septer, A.N., and Mandel, M.J. (2019). Draft genome sequences of type VI secretion system-encoding *Vibrio fischeri* strains FQ-A001 and ES401. *Microbiol. Resour. Announc.* *8*, e00385-19. <https://doi.org/10.1128/MRA.00385-19>.
46. Lyell, N.L., Colton, D.M., Bose, J.L., Tumen-Velasquez, M.P., Kimbrough, J.H., and Stabb, E.V. (2013). Cyclic AMP receptor protein regulates pheromone-mediated bioluminescence at multiple levels in *Vibrio fischeri* ES114. *J. Bacteriol.* *195*, 5051–5063. <https://doi.org/10.1128/JB.00751-13>.
47. Cecere, A.G., and Miyashiro, T.I. (2022). Impact of transit time on the reproductive capacity of *Euprymna scolopes* as a laboratory animal. *Lab. Anim. Res.* *38*, 25. <https://doi.org/10.1186/s42826-022-00135-2>.
48. Cecere, A.G., Cook, R.A., and Miyashiro, T.I. (2023). A case study assessing the impact of mating frequency on the reproductive performance of the Hawaiian bobtail squid *Euprymna scolopes*. *Lab. Anim. Res.* *39*, 17. <https://doi.org/10.1186/s42826-023-00168-1>.
49. Wasilko, N.P., Larios-Valencia, J., Steingard, C.H., Nunez, B.M., Verma, S.C., and Miyashiro, T. (2019). Sulfur availability for *Vibrio fischeri* growth during symbiosis establishment depends on biogeography within the squid light organ. *Mol. Microbiol.* *111*, 621–636. <https://doi.org/10.1111/mmi.14177>.
50. Lyell, N.L., Dunn, A.K., Bose, J.L., and Stabb, E.V. (2010). Bright mutants of *Vibrio fischeri* ES114 reveal conditions and regulators that control bioluminescence and expression of the *lux* operon. *J. Bacteriol.* *192*, 5103–5114. <https://doi.org/10.1128/JB.00524-10>.
51. Miyashiro, T., Klein, W., Oehlert, D., Cao, X., Schwartzman, J., and Ruby, E.G. (2011). The *N*-acetyl-D-glucosamine repressor NagC of *Vibrio fischeri* facilitates colonization of *Euprymna scolopes*. *Mol. Microbiol.* *82*, 894–903. <https://doi.org/10.1111/j.1365-2958.2011.07858.x>.
52. Schmittgen, T.D., and Livak, K.J. (2008). Analyzing real-time PCR data by the comparative C(T) method. *Nat. Protoc.* *3*, 1101–1108. <https://doi.org/10.1038/nprot.2008.73>.
53. Studer, S.V., Schwartzman, J.A., Ho, J.S., Geske, G.D., Blackwell, H.E., and Ruby, E.G. (2014). Non-native acylated homoserine lactones reveal that LuxIR quorum sensing promotes symbiont stability. *Environ. Microbiol.* *16*, 2623–2634. <https://doi.org/10.1111/1462-2920.12322>.

STAR★METHODS

KEY RESOURCES TABLE

REAGENT or RESOURCE	SOURCE	IDENTIFIER
Bacterial and virus strains		
Wild-type <i>V. fischeri</i>	Boettcher and Ruby; Mandel et al. ^{43,44}	ES114
T6SS2+ Wild-type <i>V. fischeri</i>	Sun et al. and Bultman et al. ^{22,45}	FQ-A001
FQ-A001 $\Delta hcp \Delta hcp1$	Guckes et al. ¹²	NPW58
FQ-A001 $\Delta litR$	This study	KRG001
ES114 $\Delta ainS \Delta luxIR P_{lux-lux}CDABEG$	Kimbrough and Stabb ³⁰	JHK007
C8 HSL bioreporter strain of <i>V. fischeri</i>	Lyell et al. ⁴⁶	DC22
<i>E. coli</i> for cloning	Lab stock	Top10
<i>E. coli</i> for cloning and conjugation into <i>V. fischeri</i>	Lab stock	S17-1 λ -pir
ES114 Tn7::erm	Miyashiro et al. ¹⁸	TIM313
FQ-A001 $\Delta vasH$	Guckes et al. ⁷	KRG005
Chemicals, peptides, and recombinant proteins		
Yeast Extract	Fisher, Hampton, NH, USA	Cat#BP1422-500
Tryptone	Fisher, Hampton, NH, USA	Cat#BP1421-500
Sodium Chloride	Fisher, Hampton, NH, USA	Cat#BP358-10
Agar	Fisher, Hampton, NH, USA	Cat#BP1423-500
Tris Base	Fisher, Hampton, NH, USA	Cat#BP152-1
<i>N</i> -octanoyl-L-homoserine lactone	Cayman Chemical, Ann Arbor, MI, USA	Cat#10011199
<i>N</i> -(3-Oxohexanoyl)-L-homoserine lactone	Sigma-Aldrich St. Louis, MO, USA	Cat#K3007-10MG
Instant Ocean Sea Salt	Fisher, Hampton, NH, USA	Cat#NC1023135
KpnI-HF	NEB, Ipswich, MA, USA	Cat#R3142S
SacI-HF	NEB, Ipswich, MA, USA	Cat#R3156S
XbaI-HF	NEB, Ipswich, MA, USA	Cat#R0145S
XmaI-HF	NEB, Ipswich, MA, USA	Cat#R0180L
Sall-HF	NEB, Ipswich, MA, USA	Cat#R3138S
T4 DNA Ligase	NEB, Ipswich, MA, USA	Cat#M0202L
Chloramphenicol	Fisher, Hampton, NH, USA	Cat#BP904100
PFU Ultra Polymerase	Agilent, Santa Clara, CA, USA	Cat#600385-51
EconoTaq Plus 2x Master Mix	Fisher, Hampton, NH, USA	Cat#NC0421795
Isopropyl- β -D-thiogalactopyranoside (IPTG)	Fisher, Hampton, NH, USA	Cat#BP162010
MuLV Reverse Transcriptase	NEB, Ipswich, MA, USA	Cat#M0253S
Oligonucleotides are listed in Table S1	N/A	N/A
Plasmids are listed in Table S2	N/A	N/A
Critical commercial assays		
Zero Blunt PCR Cloning Kit	Invitrogen, Waltham, MA, USA	Cat#K270020
EZNA Miniprep Kit	Omega Bio-tek, Norcross, GA, USA	Cat#D6943-02
Gel Extraction Kit	Omega Bio-tek, Norcross, GA, USA	Cat#D2500-01
Cycle Pure Kit	Omega Bio-tek, Norcross, GA, USA	Cat#D6492-01
RNeasy Kit	Qiagen, Hilden, Germany	Cat#74004
Turbo DNA-free Kit	Invitrogen, Waltham, MA, USA	Cat# AM1907
Software and algorithms		
Prism 9	GraphPad	Version 9.3.1
ImageJ	NIH (Public Domain)	Fiji version 2.0.0

RESOURCE AVAILABILITY

Lead contact

Further information and reasonable requests for resources and reagents should be directed to and will be fulfilled by the lead contact, Tim I. Miyashiro (tim14@psu.edu).

Materials availability

Strains and plasmids generated for this study are available upon reasonable request from the lead contact.

Data and code availability

- All data reported in this paper will be shared by the lead contact upon request.
- This paper does not report original code.
- Any additional information required to reanalyze the data reported in this paper is available from the lead contact upon request.

EXPERIMENTAL MODEL AND SUBJECT DETAILS

E. scolopes hatchlings were generated using the mariculture facility described previously.^{47,48} Briefly, egg clutches that were produced by female *E. scolopes* were maintained in individual chambers with circulating water. Upon hatching, individual hatchlings were transferred to tumblers for experimentation. All adult animals associated with the mariculture facility were collected in offshore seawater in Oahu, HI. Collection, care, and research of all laboratory animals was completed under the program's Institutional Animal Care and Use Committee (IACUC). IACUC protocol #PROTO202101789.

All *V. fischeri* strains used in this study were derived from either ES114 or FQ-A001, and regularly maintained on LBS medium (defined below) at 28°C.^{44,45} Glycerol stocks of *V. fischeri* strains were maintained at -80°C. Strains were regularly authenticated by testing for the presence of specific mutations, e.g., $\Delta litR$, by colony PCR using primers that flank the mutation.

Growth conditions

The *V. fischeri* strains and plasmids used in this report are listed in the [key resources table](#). *V. fischeri* strains were grown aerobically in LBS medium [1% (w/v) tryptone, 0.5% (w/v) yeast extract, 2% (w/v) NaCl, 50 mM Tris-HCl (pH 7.5)] or SWTO medium [0.5% (w/v) tryptone, 0.3% (w/v) yeast extract, 0.3% of glycerol in Instant Ocean mixed to 35 ppt].^{49,50} For solid medium, agar was added to a final concentration of 1.5% w/v. When growing strains harboring plasmids, the medium was supplemented with chloramphenicol (Cm) at a final concentration of 2.5 $\mu\text{g mL}^{-1}$ and/or erythromycin (Erm) at a final concentration of 5 $\mu\text{g mL}^{-1}$. When appropriate, IPTG was dissolved in water as a vehicle and used at a final concentration of 100 μM . Autoinducers (C8 HSL and 3-oxo-C6 HSL) were dissolved in DMSO as a vehicle and used at a final concentration of 1 μM .

Unless stated otherwise, starter cultures for the experiments described in this report began by inoculating for each strain 3 mL LBS containing antibiotic as appropriate with an isolated colony of the indicated strain and incubating cultures at 28°C overnight with shaking (200 rpm). Cell suspensions were then generated by normalizing culture samples to $\text{OD}_{600} = 1.0$ using LBS as a diluent. In the assays described below, these cell suspensions were used either directly in the assay or to generate cultures by diluting 1:100 into the indicated medium in either culture tubes or Erlenmeyer flasks. In this study, LCD and HCD correspond to OD_{600} ranging from 0.1 to 0.3 and 2.0–2.6, respectively. To generate spent media, culture samples were cooled quickly on ice and centrifuged at 4°C at 3,220 $\times g$ for 7 min. The resulting supernatant was filtered through a 0.22- μm filter and stored at 4°C until being used.

METHOD DETAILS

Molecular Biology

The deletion allele $\Delta litR$ was generated using FQ-A001 genomic DNA by PCR amplification of 1.5-kb regions flanking *VFFQA001_RS16675* and cloning the products into pEVS79, generating the mutagenesis construct pKRG002. Primers and restriction sites used in the cloning process are listed in [Table S2](#). To generate the knockout mutant, this plasmid was introduced into FQ-A001 by conjugation and screening by PCR for the double-crossover event, according to a previously established protocol.¹⁸

Construction of promoter reporters was accomplished by amplifying specific promoter regions from FQ-A001 genomic DNA using the primers listed in the [key resources table](#). The amplicon was cloned into the pCR-Blunt vector (Invitrogen) and verified by sequencing. The insert was subcloned into pTM267 using XbaI and XmaI to generate a GFP transcriptional fusion.¹⁸

The inducible *litR* construct was generated by amplifying the *litR* gene from FQ-A001 using the primers listed in the [key resources table](#). The amplicon was cloned into the pCR-Blunt vector (Invitrogen), confirmed by sequencing, and isolated using XmaI and Sall (NEB) restriction enzymes. The insert was subsequently cloned downstream of the P_{trc} IPTG-inducible promoter using the XmaI/Sall-derived vector fragment of pTM214.⁵¹

Co-incubation assays

Co-incubation assays consisted of mixtures of FQ-A001-derived cells with either ES114 harboring pYS112, which expresses CFP, or the ES114-derived strain TIM313, which contains a chromosomally integrated *erm^R* marker at the Tn7 site. To control for potential variation among the ES114-derived strains in co-incubation assays, cultures of pYS112/ES114 and TIM313 were grown in SWTO-Cm and SWTO, respectively, to $OD_{600} = 1.0$, at which point they were chilled on ice, mixed with glycerol to 25% (v/v), dispensed as 0.5-mL aliquots, and frozen at -80°C . Prior to initiating an assay, aliquots were thawed on ice.

To initiate a co-incubation assay, a 50- μL cell suspension of an FQ-A001-derived culture was combined with 50 μL of an ES114-derived strain in a microfuge tube and briefly vortexed. A 10- μL volume was placed onto the surface of LBS agar, with up to six different samples per Petri dish, with biological replicates on different petri dishes. Petri dishes were incubated at 24°C and assessed at the indicated time. For experiments involving multiple time points, one sample was prepared for each time point.

To assess the CFP fluorescence within a sample that included pYS112/ES114, an image of the spot was acquired in RAW format using a Rebel T5 Camera (Canon) mounted on a SZX16 fluorescence dissecting microscope (Olympus) equipped with an SDF PLFL 0.3x objective and a CFP filter set. Images were processed by converting the RAW image format to TIFF using ImageJ (v. 1.52a (NIH)) digital camera raw (DCRaw macro) with the following settings: `use_temporary_directory`, `white_balance = [Camera white balance]`, `do_not_automatically_brighten`, `output_colorspace = [sRGB]`, `read_as = [8-bit]`, `interpolation = [High-speed, low-quality bilinear]`, and `half_size`. The blue channel of each image was used to show the CFP fluorescence associated with each spot.

To assess the abundance of *erm^R* CFU within a sample that included TIM313, an agar plug containing the spot was excised using flame-sterilized forceps, suspended in 1 mL LBS medium, serially diluted, plated onto LBS-Erm, and incubated at 28°C . The resulting CFU counts were used to calculate the abundance of TIM313 at the time of harvest.

Bioluminescence assay

Strain DC22 was used as a biosensor for C8 HSL. A culture of DC22 was grown by diluting a starter culture 1:1000 into a 500-mL Erlenmeyer flask containing 100 mL SWTO and growing it at 28°C at 200 rpm. At $OD_{600} = 0.8$, the culture was centrifuged at $4,000 \times g$ for 15 min. The supernatant was removed by pipetting, and the pellet was resuspended in SWTO at 1:10 the original culture volume. Each sample was prepared by combining 1.8 mL of a cell-free supernatant with 0.2 mL of the concentrated biosensor cell suspension and incubated at 28°C shaking at 200 rpm. After 20 min, a 100- μL sample was transferred to a cuvette and the corresponding bioluminescence was measured using a GloMax 20/20 luminometer (Promega). The turbidity was determined by adding 0.9 mL SWTO to the cuvette and measuring OD_{600} using a BioPhotometer spectrophotometer (Eppendorf). To construct a standard curve for using DC22 as a biosensor for C8 HSL, spent medium was generated from a culture of DC22 was first grown in 20 mL SWTO to $OD_{600} = 2.0$ as described above.

Reverse transcriptase-Quantitative PCR (RT-qPCR)

For the experiment shown in Figure 1F, cultures of FQ-A001 were grown in SWTO supplemented with C8 HSL or vehicle to LCD. The volume of sample that was harvested from each culture was equivalent to the volume of cells needed to generate an $OD_{600} = 1.0$ in 1 mL. To accomplish this, the cells were centrifuged at $3,320 \times g$ for 7 min and all but 1 mL of the supernatant was removed. The pellet was re-suspended and centrifuged again at $9,000 \times g$ for 2.5 min, after which all but 50 μL of supernatant was removed. Cell pellets were snap frozen in a 70 percent ethanol bath supercooled by dry ice and then stored at -80°C .

For the experiment shown in Figure 2C, cultures of FQ-A001 (WT) or KRG001 ($\Delta litR$) harboring either pTM214 (vector) or pKRG023 (*P_{trc::litR}*) were grown in SWTO-Cm supplemented with 100 μM IPTG to HCD. The volume of sample that was harvested from each culture was equivalent to the volume of cells needed to generate an $OD_{600} = 1.0$ in 1 mL. These cells were centrifuged at $9,000 \times g$ for 2.5 min, after which all but 50 μL of supernatant was aspirated. Cell pellets prepared for storage at -80°C as described above.

RNA extraction was performed using the Rneasy mini kit (Qiagen) according to manufacturer instructions. For each sample, 1 μg of RNA was treated with DNase using the TURBO DNA-free kit (Invitrogen) according to manufacturer instructions, and reaction products were confirmed to be free of DNA by PCR using primers specific for *rpoD*. cDNA was generated by treating 700 ng of RNA with MuLV reverse transcriptase (NEB) and random hexamers (ThermoFisher) according to manufacturer instructions. For each gene target, 50 ng of cDNA template was amplified by qPCR with an AriaMx real-time thermocycler in 20- μL reactions containing Evagreen dye (Biotium), EconoTaq Plus 2x master mix (Lucigen), and primer sets listed in Table S2. The thermocycler profile for the amplification included a 10-min hot start at 95°C followed by 40 cycles of incubation at 95°C for 15 s, 50.5°C for 45 s, and 72°C for 30 s. PCR amplicon identity was verified by heating from 55°C to 95°C with ramp time of 15 s. Relative fold changes were determined using the $\Delta\Delta\text{CT}$ method, with expression normalized using housekeeping gene *rpoD*.⁵² The ability to distinguish between *hcp* and *hcp1* is limited by the sequence similarity between the two genes.

GFP-based promoter reporter assays

To initiate the assay, a 2.5- μL volume of a cell suspension derived from a starter culture was placed on LBS-Cm agar and incubated at 24°C for 24 h. Images of each spot of growth were acquired in RAW format using a Rebel T5 Camera (Canon) mounted on a SZX16 fluorescence dissecting microscope (Olympus) equipped with an SDF PLFL 0.3x objective and both GFP and mCherry filter sets. Images were processed by converting the RAW image format to TIFF using ImageJ (v. 1.52a (NIH)) digital camera raw (DCRaw macro) with the following settings: `use_temporary_directory`, `white_balance = [Camera white balance]`, `do_not_automatically_brighten`, `output_colorspace = [sRGB]`, `read_as = [8-bit]`, `interpolation = [High-speed, low-quality bilinear]`, and `half_size`. The red channel of the

image taken using the mCherry filter was used to determine the mCherry fluorescence. mCherry signal was used to define the region of interest (ROI) via thresholding. The mean green fluorescence level within each ROI was determined using the green channel for the image taken with the GFP filter. Autofluorescence levels were determined from the pixel values associated with the green channel of an image of a non-fluorescent strain, FQ-A001 harboring plasmid pVSV105 taken using the GFP filter set.

Endpoint RT-PCR

To initiate the assay, three 10- μ L volumes of cell suspension derived from a starter culture were placed on LBS and incubated at 24°C. After 22 h, the spots of growth were scraped up from the surface using a sterile wooden stick and collectively resuspended in 1 mL LBS. A 0.9-mL volume of the cell suspension was subjected to RNA extraction and DNase treatment using the RNA Extraction Kit (Epicentre). To generate cDNA, 1.0 μ g of RNA was subjected to reverse transcription using MuLV-RT and random hexamer primers from the cDNA Synthesis Kit (ThermoFisher). For each 50- μ L PCR, 1 μ L of cDNA was used as template with PFU Ultra Polymerase and a thermocycler profile initiating with a 2-min 95°C step, followed by 30 cycles of incubation at 95°C for 30 s, 55°C for 30 s, and 72°C for 30 s, and ending with 72°C for 5 min. Primers are listed in the Oligonucleotides table. PCR products were evaluated using gel electrophoresis with 2.0% agarose gel.

Squid-colonization assays

Cultures of the indicated strains were harvested at $OD_{600} \sim 1.0$, and cells were washed twice by centrifugation at 5,000 $\times g$ for 2 min, removal of the supernatant, and re-suspension with filter-sterilized seawater (FSSW) with each wash. The cell suspension was further diluted into 50 mL FSSW, which was poured into a tumbler with 50 mL FSSW and hatchlings, with targeted inoculum sizes of 5,000 CFU/mL for FQ-A001 and 50,000 CFU/mL for ES114. Relative to parental strains, inoculums for KRG001 (FQ-A001 $\Delta litR$) and JHK007 (ES114 *luxI ainS*) were increased 5-fold and 1.5-fold, respectively, due to colonization defects associated with each strain. Hatchlings used in these experiments were less than 24 h old and generated by a mariculture facility as described elsewhere.⁴⁷ Delayed inoculation experiments were performed by generating inoculums initially with only ES114-derived strains and then adding FQ-A001-derived cells 1 h later. After 3.5 h of exposure to ES114 cells, animals were washed of the inoculum by being transferred to 100 mL fresh FSSW twice. After washing, each squid was singly housed in an individual vial containing 4 mL FSSW. For animals that were exposed to C8 HSL treatment, 1 μ M C8 HSL, which was diluted in dimethylsulfoxide (DMSO) as a solvent, was added to the 4 mL FSSW in which animals were housed overnight. This concentration of C8 HSL is less than the 5 μ M used to complement the *ainS* mutant of ES114 *in vivo* as previously described.⁵³ DMSO was used as a vehicle-only control and previous work has shown 0.25% DMSO does not impact squid physiology.⁵³ At 24 h post-inoculation (pi), animals were transferred to new vials containing 4 mL FSSW and evaluated for bioluminescence using GloMax 20/20 luminometer (Promega). Immediately afterward, animals were placed on ice for 10 min, fixed in 4% paraformaldehyde, and imaged by fluorescence microscopy with a Zeiss 780 confocal microscope (Carl Zeiss AG, Jena, Germany).¹¹

QUANTIFICATION AND STATISTICAL ANALYSIS

Statistical details of experiments, including the statistical test(s) used to determine significance and how significance is represented in each plot, can be found in the figure legends and in the main text. For culture-based experiments, each circle represents an independent biological replicate. For animal experiments, samples were randomized prior to imaging and analysis. Each plot displayed in this manuscript is representative of at least two experimental trials. Plots were generated and statistical tests were performed using GraphPad Prism (v 9.5.1).